Docking and MD study of histamine H4R based on the crystal structure of H1R

Zhiwei Feng, Tingjun Hou, Youyong Li*

Institute of Functional Nano & Soft Materials (FUNSOM) and Jiangsu Key Laboratory for Carbon-Based Functional Materials & Devices, Soochow University, Suzhou, Jiangsu 215123, China

ARTICLE INFO

ABSTRACT

Histamine H4 receptor (H4R), a member of histamine receptor family, which belongs to class A of G-protein coupled receptors (GPCRs), has been reported to play a critical role in histamine-induced chemotaxis in mast cells and eosinophils. Recently, the crystal structure of human histamine H1 receptor (H1R) was reported, which facilitates structure-based drug discovery of histamine receptor significantly. In the current work, the homology models of H4R and H3R are first constructed based on the crystal structure of H1R. Clobenpropit is then docked into the binding pocket of H4R and two different binding modes can be identified. In order to select a reasonable binding mode, several other ligands including agonists and antagonists are docked into H4R, and the results reveal that all ligands share one preferable binding mode: the protonated —NH tightly interacts with Asp$^{3.32}$ and the imidazole —NH interacts with Glu$^{5.46}$. By comparing H3R and H4R, we find that Glu$^{5.20}$ and Thr$^{6.55}$ in H4R involve in the selectivity of H4R. Then, we perform molecular dynamics (MD) simulations for H4R in complex with its compounds. MD results indicate that the preferable docking mode is more stable. Finally, we dock agonist histamine into H1R and H4R, and then perform 20 ns MD simulations for the complexes. H1R or H4R bound with histamine show strong conformational changes from TM5, TM6 and TM7, outward movement of intracellular part of TM6, and conformational change of Tyr$^{7.53}$, which is consistent with the recent crystal structures of active GPCRs. Our results reveal the mechanism of selectivity and activation for H4R, which is important for developing selective antagonists and agonists for H4R.

© 2012 Elsevier Inc. All rights reserved.

1. Introduction

Histamine [1–7], a chemical messenger, exerts many numerous physiological processes in hypersensitivity responses, gastric acid secretion, neurotransmission, immunomodulation, cell differentiation, and embryonic development through four distinct receptors: H1R, H2R, H3R and H4R, which belong to class A of G-protein coupled receptors (GPCRs) [8–14]. H1R [6,15–19] mainly expresses in nerve cells, hepatocytes, chondrocytes, endothelial cells, airway and vascular smooth muscles, epithelial cells, neutrophils, eosinophils, monocytes, marcophages, DC, T and B cells. H1R mediates many pathological processes, which include allergenic rhinitis, atopic dermatitis, conjunctivitis, urticaria, asthma, anaphylaxis, bronchoconstriction and enhanced-vascular permeability in the lung. H1R is pharmacologically identified and has been successful blockbuster targets for more than two decades.

H3R [20–28] mainly presents in nervous system, involving in cognition, sleep–wake status, energy homeostatic regulation and inflammation. H3R modulates the release of various neurotransmitters in the central and peripheral nervous system and therefore is a potential target in the therapy of numerous diseases. In recent years, many ligands [29] of H3R have rapidly increased, including immepip, imetit, R-α-methylhistamine, burimamide, clobenpropit, thioperamid, immethridine, JNJ6379490 and A349821.

H4R [7,24,29–32] mainly distributes in hematopoietic cells, and plays a key role in nociceptive responses, autoimmune disorder, allergic conditions, colon cancer, and breast cancer. Interestingly, most antagonists and agonists of H1R and H2R do not bind to H4R, while ligands (like thioperamid, clobenpropit, imetit and R-α-methylhistamine) of H3R can bind into H4R. H4R can be activated by many ligands belonged to H3R. Recently, JNJ 7777120 [33] ($K_i = 20$ nM) and related benzimidazole analog VUF 6002 ($K_i = 79$ nM) are identified as selective and potent H4R antagonists [29].

A sequence alignment [29] of H1R, H3R and H4R shows human H4R shares high sequence similarity with H3R. At a protein level, H4R and H3R share 38% sequence identity and 53.6% sequence similarity. While in the trans-membrane domain, they share up to 54% sequence identity. However, H1R only shares ~20% sequence identity with H3R and ~23% sequence identity with H4R, which is higher than other known crystal structures of GPCRs [29]. Considering the

high sequence identity and sequence similarity between H3R and H4R, we are not surprising that H4R can be activated by H3R agonists. The near-identity of the residues inferred to form the binding site between H4R and H3R produces a formidable challenge to develop H4R-selective compounds with drug-like physicochemical properties. It is a great challenge to identify the selective histamine H4R ligands with high binding affinities and understand the pharmacological role of H4R.

Recently, the crystal structure of human histamine H1R was reported [18]. The authors first docked a first-generation antagonist-doxepin into H1R and found ligand sited deep in ligand-binding pocket and directly interacted with Trp$^{6.48}$. Then they docked several second-generation H1R antagonists into H1R and found the unique carboxyl group presented in this class of ligand interacted with Lys$^{5.39}$, which was not conserved in other aminergic receptors, demonstrating how minor differences in receptors leaded to pronounced selectivity differences with small molecules. All these make structure-based methodologies plausible to develop high selective compounds for H1R and help us further understand the pharmacological role of other aminergic receptors.

In the present work, we construct H4R and H3R based on the crystal structure of H1R and dock clobenpropit into H3R and H4R. In the complex of H4R with clobenpropit, we find two different binding modes. Then we dock several ligands including agonists and antagonists into H4R, and find that most of them share one similar binding mode. Then we perform 20 ns molecular dynamics (MD) Simulations of both two binding modes in H4R, and agonist-bound/antagonist-bound both of H1R and H4R. Our results provide structural information for developing high selective antagonists and agonists for H4R.

2. Methods

2.1. Homology modeling

The crystal structure of human histamine H1R [18] (PDB entry: 3RZE, resolution 3.10 Å) is prepared by Discovery Studio [34] (including residues repair and energy minimization). The missing loop between TM4 and TM5 (residues 168–174) is built by Discovery Studio. Fig. S1 shows a homology model superimposed with the crystal structure, which the RMSD is less than 0.5 Å.

The crystal structure of H1R is then used as a template to construct H3R and H4R. The sequences of human H3R and H4R are retrieved from GenBank (Q9Y5N1 and Q9H3N8) (http://www.uniprot.org/uniprot/). Then we build the homology models of H3R and H4R by using Discovery Studio [34]. The models of H3R and H4R have two disulfide bonds and one disulfide bond, respectively. The disulfide bonds of H3R consist of Cys73–Cys154 and Cys350–Cys354, while the disulfide bond of H4R consists of Cys72–Cys149. Fig. S2 shows a sequence alignment for H1R, H3R and H4R.

Once the 3D models are generated, energy minimization is performed for the receptors before dockings and molecular dynamics simulations. Structural evaluation and stereochemical analyses are performed by using proSA-web Z-scores [35] and PROCHECK Ramachandran plots [36]. Furthermore, Root Mean Squared Deviation (RMSD), superimposition of query and template structure, and visualization of generated models are performed using UCSF Chimera 1.5.3 [37].

2.2. Ligands preparation

In the present study, we use several ligands including agonists and antagonists. We first docked these ligands into the receptors, and then use Discovery Studio 2.5 to predict the complex ionization

and residue pK values, especially the protonation states of ligands. For example, the NH group in clobenpropit is protonated by Discovery Studio program due to the strong interaction of residue Asp$^{3.32}$ or Glu$^{5.46}$, thus carrying a positive charge. The protonation states are shown in Table 1 and the partial charges of the ligands are shown in Fig. S8.

2.3. Construction for the 3D model of receptor-ligand complex

The dock program CDocker and Discovery Studio [34] Catalyst Score are applied to construct receptor-ligand complexes. The center of the binding site of the receptor is set at the center of ligand in the crystal structure of human histamine H1R with a radius of 13 Å, large enough to cover the binding pocket. CDocker [34] is a grid-based molecular docking method that employs CHARMM [38–40]. Receptor is held rigid while ligands are allowed to flex during the refinement. For pre-docked ligands, prior knowledge of the binding site is not required. It is possible, however, to specify the ligand placement in the active site using a binding site sphere. Random ligand conformations are generated from the initial ligand structure through high temperature molecular dynamics, followed by random rotations. The random conformations are refined by grid-based simulated annealing and a final grid-based or full force field minimization. The RMSD of our docking structure of H1R with doxepin by using CDocker [34] compared to the crystal structure is 1.21 Å, more details can be found in Supplementary Fig. S3.

2.4. MD Simulations

The complex of receptor with ligand is embedded in a pre-equilibrated and periodic structure of 1-palmytoil-2-oleoylsn-glycero-3-phosphatidylcholine (POPC) by using VMD [41] program. The lipid molecules within 5 Å of the complex are eliminated. Then we insert it into a water box (TIP3P [42] water model) and eliminate the waters within 5 Å of the lipid and protein. The whole system is built up by using VMD [41,43] program.

The whole system (Fig. 1) contains protein, 116 lipid molecules, 7783 water molecules, and 5 chlorine ions for a total of 43,326 atoms per periodic cell. The box size is 80 Å by 80 Å by 90 Å. The system is first equilibrated for 500 ps with the protein fixed. Then the protein is released and another 500 ps equilibration is performed.

Starting from the last frame of the equilibration, our simulations are initiated. Our MD simulations are performed by using NAMD [44] package version 2.7b2 with CHARMM [38–40] force field for each receptor-ligand complex with explicit water and a periodically infinite lipid. In addition, Dreiding force field is used to describe the ligand and ligand/protein interactions. Electrostatics calculation is done by using the particle mesh Ewald (PME) method [45] with a 12 Å non-bonded cutoff. The van der Waals energies are calculated using a smooth cutoff (switching radius 10 Å, cutoff radius 12 Å). The temperature and pressure are kept constant using a langevin thermostat and langevin barostat, respectively. The time step of MD simulations is set to 1 fs. The data is saved every 10 ps for analysis. Finally, 20 ns MD simulation is performed under a constant temperature of 310 K and a constant pressure of 1 atm. Trajectory analyses are carried out with VMD [41,43].
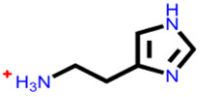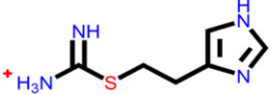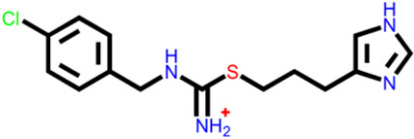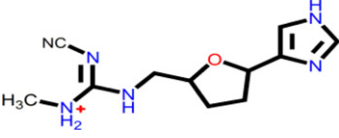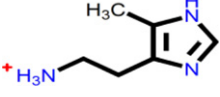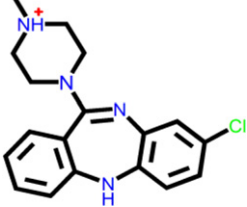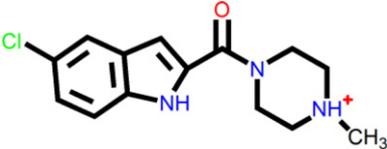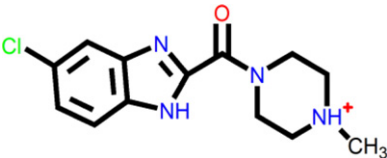
3. Results and discussion

3.1. Membrane thickness

In the molecular modeling study of a lipid bilayer, the cross-sectional area per lipid and the membrane thickness are adequate indicators of the bilayer thermal equilibration.

Bilayer thickness is evaluated as the distance between the average positions of phosphorus atoms in the two leaflets of a bilayer.

Table 1
Structure of ligands and effect concentration.

Ligand	Chemical structure	H_4	H_3
Histamine[a]		$K_i = 5$ nM	$K_i = 3.1$ nM
Imetit[b]		$K_i = 5$ nM	$K_i = 0.5$ nM
Clobenpropit[c]		$K_i = 13$ nM	$K_i = 84.7$ nM
Oup16[d]		$K_i = 125$ nM	$K_i = 0.611$ nM
4-Methylhistamine[e]		$K_i = 50$ nM	$K_i = 2000$ nM
Clozapine[f]		$K_i = 6.7$ nM	–
JNJ7777120[g]		$K_i = 20$ nM	$K_i = 2000$ nM
VUF6002[h]		$K_i = 79$ nM	$K_i = 3950$ nM

We choose eight ligands including 6 agonists and 2 antagonists. Agonists include: (a) histamine, (b) imetit, (c) clobenpropit, (d) Oup16, (e) 4-methylhistamine, and (f) clozapine. Antagonists include: (g) JNJ7777120 and (h) VUF6002.

The average phosphorus–phosphorus distance in the POPC bilayer is 38.8 Å. Average cross-sectional area/POPC is ∼61.4 Å^2 in POPC bilayer. The values of cross-sectional area per lipid and the membrane thickness are in agreement with the recent study [46], which indicate that our system is equilibrated. Snapshot of the POPC bilayer at the end of the respective 20 ns trajectory is shown in Fig. 2.

3.2. Two different binding modes in H4R

First, we dock clobenpropit [47–49] into H4R and find that there are two different binding modes, which is in agreement with the recent study [50]. The mutational data [51–55] of H4R has reported that histamine has two major anchoring points: Asp$^{3.32}$ and Glu$^{5.46}$.

Fig. 3a illustrates that the imidazole −NH of clobenpropit interacts with Asp$^{3.32}$ while the protonated part (−NH) of clobenpropit forms hydrogen bond with Glu$^{5.46}$. Differently, as in Fig. 3b, the protonated part (−NH) of clobenpropit interacts with Asp$^{3.32}$ while the imidazole −NH forms hydrogen bond with Glu$^{5.46}$. These two binding modes are found in our docking, which is in agreement with the recent study from Istyastono [56].

Jojart et al. [52] has analyzed the binding mode of H4R by using homology model based on the crystal structure of bovine rhodopsin [57]. The H-bonding surfaces of the binding site of histamine show Asp$^{3.32}$ and Glu$^{5.46}$ are hydrogen accepting site, and the protonated ethylamine and −NH moieties of histamine are two potential hydrogen donor groups. Therefore, there are two possible binding modes of histamine at the binding site. However, they chose the
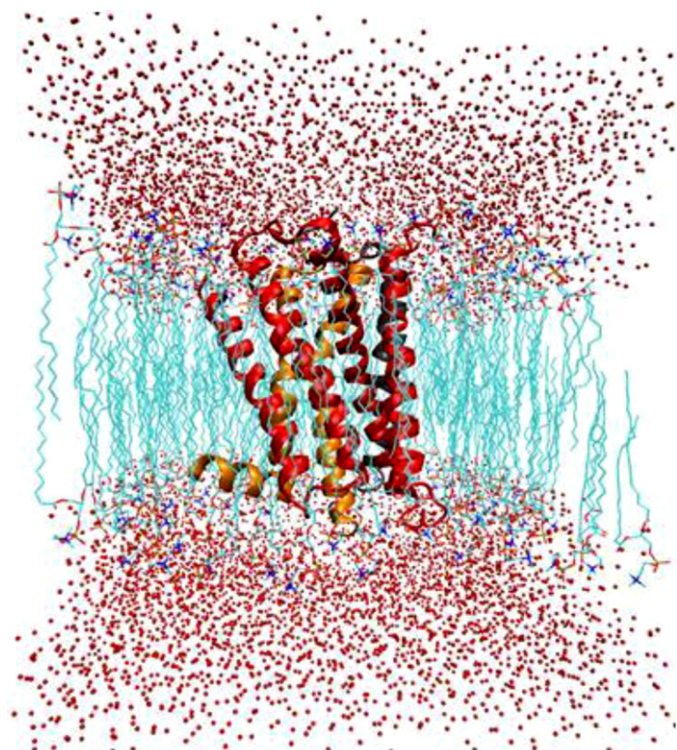
3.3. Binding of agonists and antagonists of H4R

In order to further study the binding mode of H4R, after minimization of H4R and its compounds, which include histamine, imetit, clobenpropit, OUP16, 4-methylhistamine, clozapine, JNJ 7777120, and VUF 6002, we use CDocker program in Discovery Studios [34] to dock ligands (Table 1) into H4R.

Fig. S4 (Supplementary Fig. S4) illustrates the binding modes of eight ligands including 6 agonists and 2 antagonists with different shapes, which may involve in most of the binding pockets.

First, our results show that all protonated ethylamine sides and other protonated parts (−NH) interact with $Asp^{3.32}$ in H4R. The imidazole −NH of agonists interacts with $Glu^{5.46}$, which is supported by many docking results and mutational results [51–55]. Differently, in the binding mode of antagonist-bound, our results show that the imidazole −NH of antagonists forms hydrogen bond with $Tyr^{3.33}$. However, the hydrogen bond distance between the imidazole −NH of antagonists and $Glu^{5.46}$ is within 4.5 Å. It is a significant difference between agonist and antagonist of H4R. All the binding modes of eight ligands are similar to our second mode (mode 2) in Section 3.2, which solidifies that our second mode (mode 2) is more reasonable.

Moreover, these binding modes (similar to mode 2) are also similar to that in H1R and H2R [51] as described in the previous section. Although, H4R has less sequence identity and sequence similarity with H1R and H2R as with other GPCR [58], the tight interaction with the highly conserved $Asp^{3.32}$ is common in these receptors.

Our results are also supported by docking results of H3R [23,28,59], mutant results and docking results of H4R [53,60]: Jongejan et al. [53] carried out single point mutations by using JNJ 7777120 at 3.32 (D3.32A and D3.32Q) and 5.46 (E5.46A and E5.46Q) and found binding of both radiolabels was completely abolished by both mutations at position 3.32 and E5.46A mutant, whereas JNJ 7777120 [31,33] was hardly affected by E5.46Q mutation. Their binding mode [53] is similar to our second mode. Meanwhile, our second binding mode (mode 2) is also supported by the results from Igel et al. [60].

Finally, according to the crystal structures including $A_{2A}AR$ [61,62], $β_2AR$ [63,64], D3R [65], CXCR4 [66], and histamine H1R

Fig. 1. The molecular dynamics simulation box of H4R with lipid and water. The snapshot shown above is after 20 ns simulation. The EC region is at the top.

binding mode which is very similar to our first binding mode (mode 1: the ethylamine part interacts with $Glu^{5.46}$, while the imidazole −NH interacts with $Asp^{3.32}$).

However, our second binding mode (mode 2) is similar to that in H1R and H2R [51]. Site-directed mutagenesis studies [51] reveal the protonated ethylamine function of histamine forms a hydrogen bond to highly conserved $Asp^{3.32}$.

In the following sections, we dock more ligands into H4R to differentiate the two binding modes.

Fig. 2. Snapshot of the POPC bilayer at 20 ns of MD simulation.
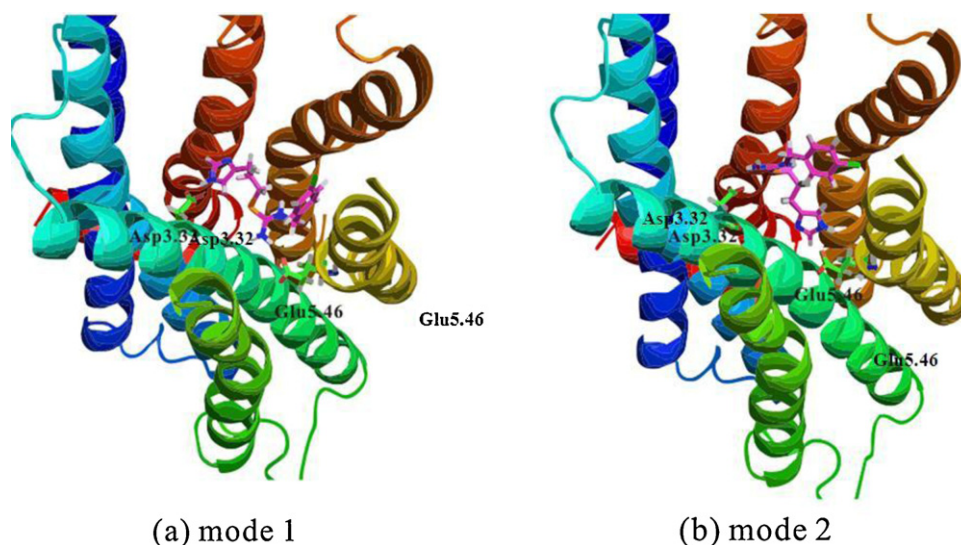
(a) mode 1   (b) mode 2

Fig. 3. Two different binding modes of clobenpropit with H4R. (a) Mode 1: the imidazole ─NH interacts with Asp[3.32] while the protonated part (─NH) of clobenpropit forms hydrogen bond with residue Glu5.46. (b) Mode 2: the protonated part (─NH) of clobenpropit interacts with Asp[3.32] while the imidazole ─NH forms hydrogen bond with residue Glu5.46.

[18], other groups' mutant results and the docking results of H4R [51,53,60], we find that the protonated ethylamine and other protonated parts tightly interact with highly conserved residues Asp[3.32], which is in agreement with our second binding mode (mode 2).

3.4. Comparison of binding pocket between H3R and H4R

There are high sequence identity and sequence similarity between H3R and H4R. H4R can be activated by many H3R agonists, including immepip, imetit. It is a challenge to identify selective
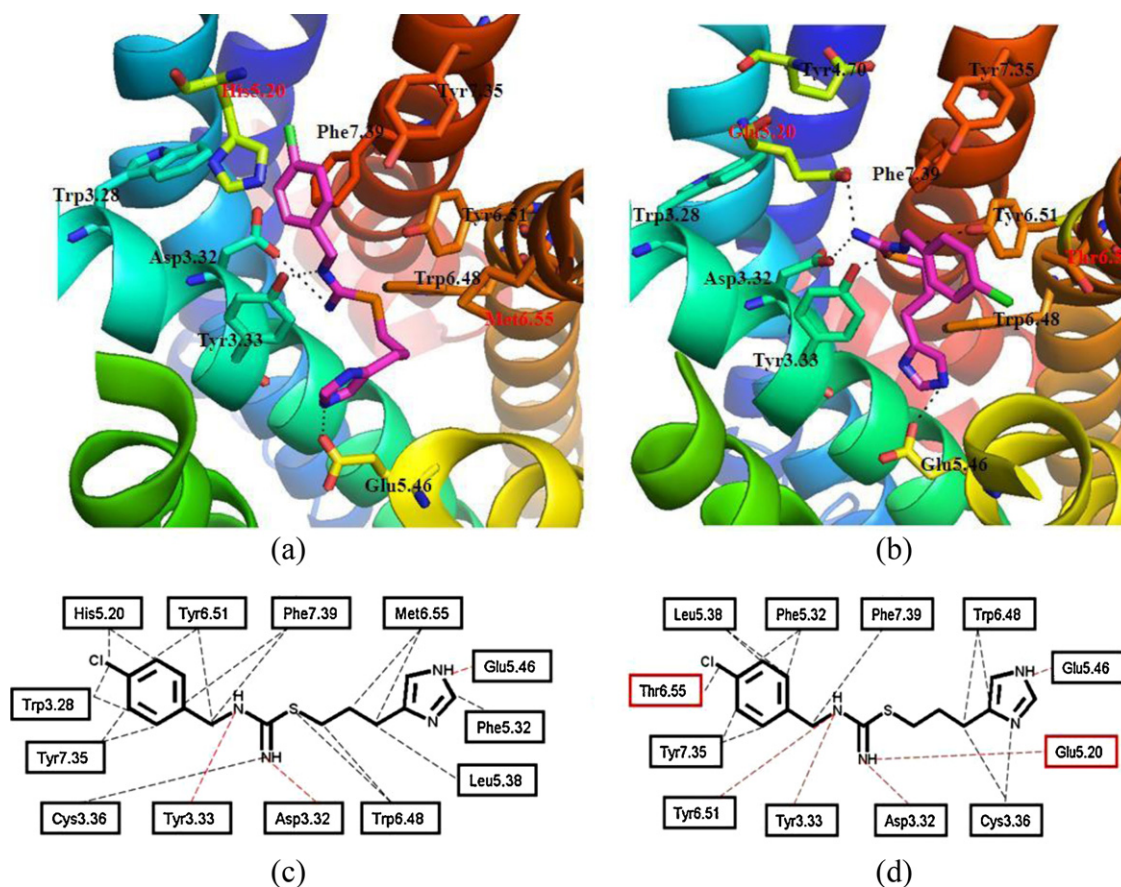
Fig. 4. (a) The binding mode of clobenpropit with H3R. (b) The binding mode of clobenpropit with H4R. (c) Schematic view of the interactions between clobenpropit and H3R: hydrophobic contacts are shown in gray dashed lines, and hydrogen bonds are highlighted in red and (d) Schematic view of the interactions between clobenpropit and H4R: hydrophobic contacts are shown in gray dashed lines, and hydrogen bonds are highlighted in red. The different residues for H4R are highlighted in red.

Fig. 5. (a) The binding pose of doxepin with H1R after 20 ns MD and (b) Time evolution of hydrogen bond distances between doxepin and H1R during 20 ns molecular dynamics.
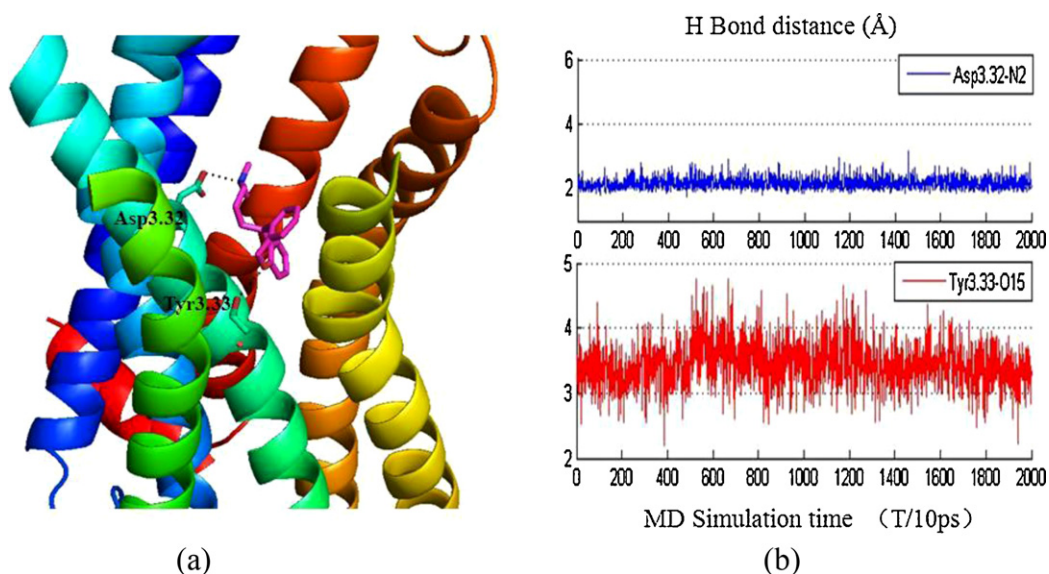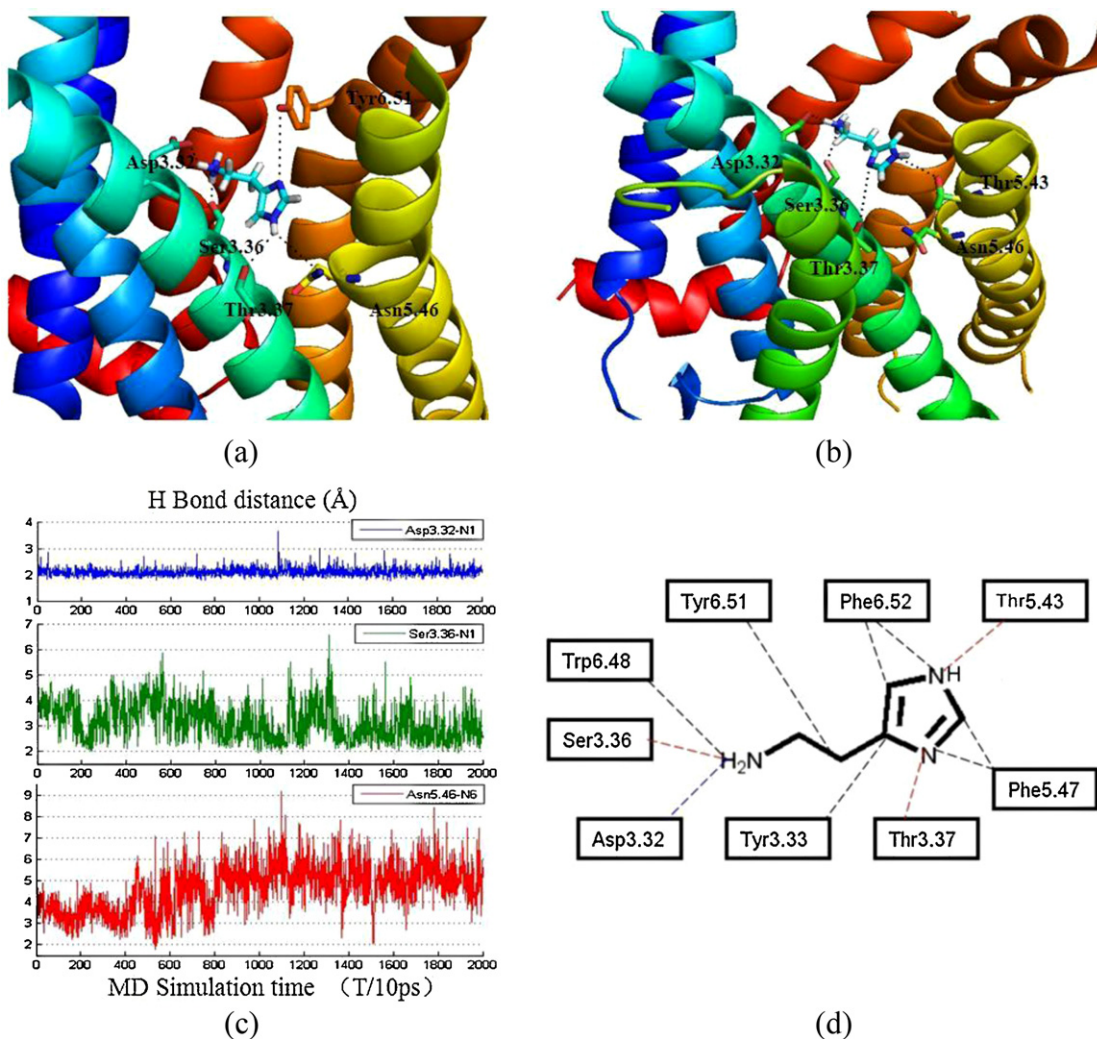

Fig. 6. (a) The hydrogen bonds formed between histamine and H1R before MD. (b). The hydrogen bonds formed between histamine and H1R after 20 ns MD. (c) Time evolution of hydrogen bond distances between histamine and H1R during 20 ns molecular dynamics and (d) Schematic view of the interactions histamine and H1R after 20 ns MD: hydrophobic contacts are shown in gray dashed lines, hydrogen bonds are highlighted in red, and salt bridges are highlighted in blue. We can see more hydrogen bonds form during our MD. (For interpretation of the references to color in this figure legend, the reader is referred to the web version of the article.)

Fig. 7. (a) The hydrogen bonds formed between clobenpropit and H4R in mode 1 after 22 ns MD. Asp[3.32] does not form hydrogen bond with the ligand. (b) The hydrogen bonds formed between clobenpropit and H4R in mode 2 after 20 ns MD and (c) Time evolution of hydrogen bond distances of mode 1 and mode 2 between clobenpropit and H4R during 20 ns molecular dynamics.
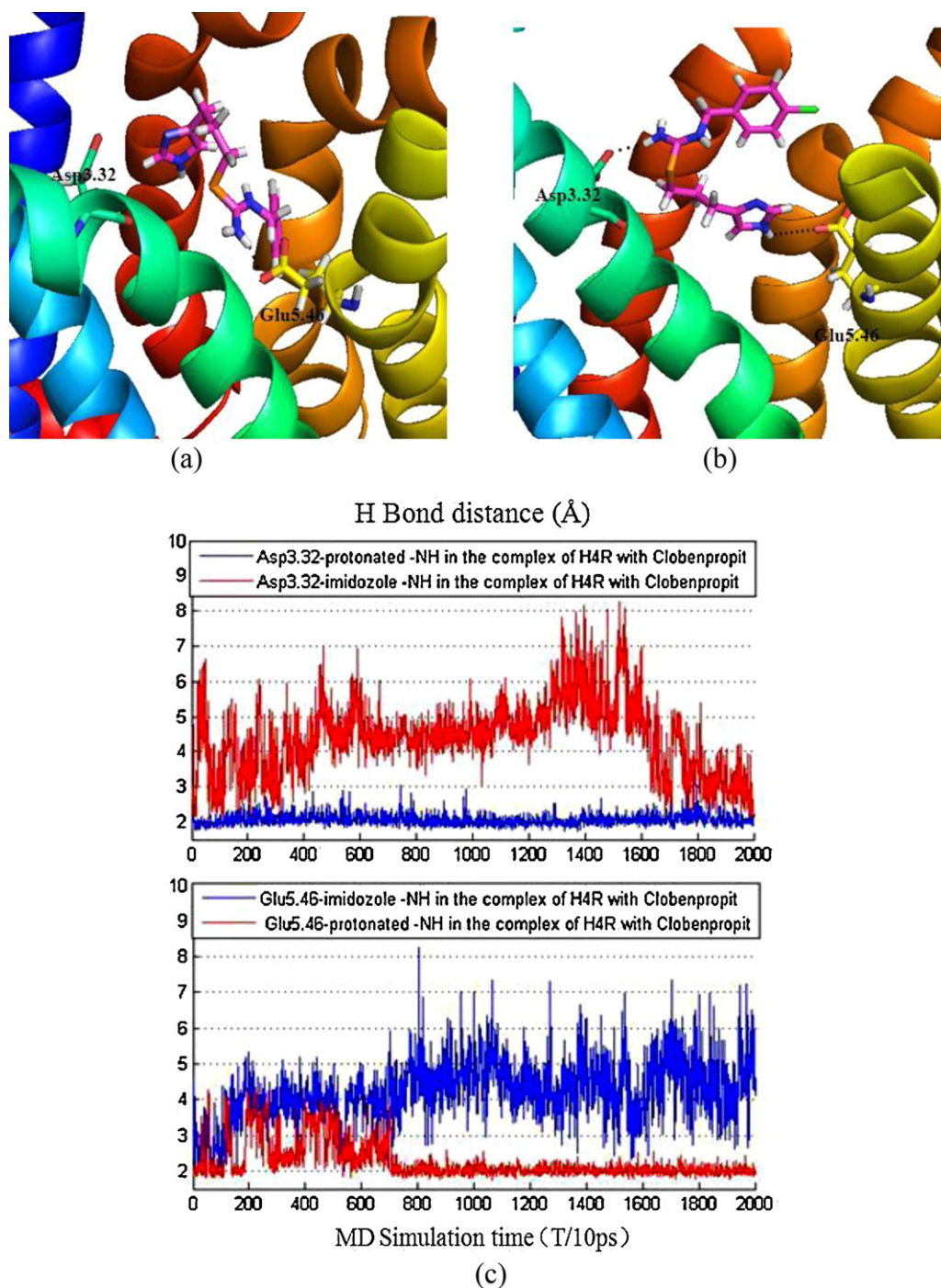
histamine H4R ligands with high binding affinities [67–70]. In order to further study the differences of binding pocket between H3R and H4R, we dock clobenpropit into H3R, and we compare the binding mode of H3R and H4R systematically to identify the differences.

Fig. 4a and b illustrates the binding mode of clobenpropit with H3R and with H4R. Fig. 4c and d illustrates their interactions.

As shown in Fig. 4a, His[5.20] from ECL2, Trp[3.28] and Phe[7.39] lock the binding pocket, so clobenpropit locates among TM2, TM3, TM5,

TM6, TM7 and ECL2. Residues including Asp[3.32], Tyr[3.33] and Glu[5.46] in H3R form hydrogen bonds with clobenpropit.

However, as shown in Fig. 4b, clobenpropit locates among TM3, TM5, TM6, TM7 and ECL2. Asp[3.32], Tyr[3.33] and Glu[5.46] in H4R also form hydrogen bonds with clobenpropit. Differently, Glu[5.20] from ECL2 and Tyr[6.51] also form hydrogen bonds with clobenpropit.

Moreover, our results show that most residues involved in the binding pocket of H3R or H4R are the same, which include Asp[3.32], Tyr[3.33], Cys[3.36], Phe[5.32], Leu[5.38], Glu[5.46], Trp[6.48], Tyr[6.51], Tyr[7.35] and
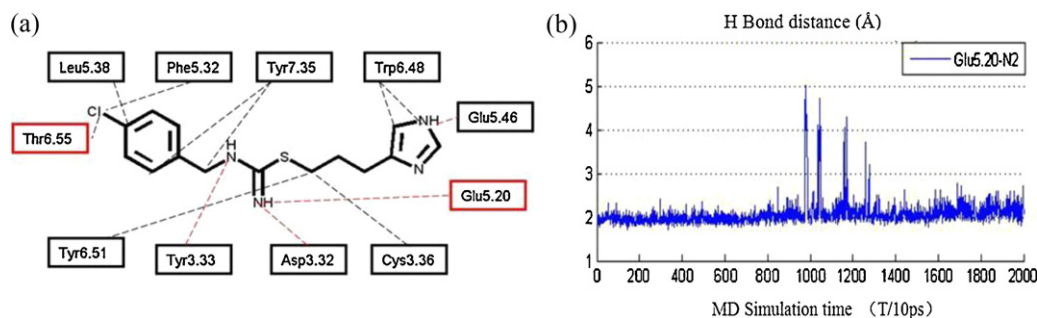
Fig. 8. (a) Schematic view of the interactions between clobenpropit and H4R in mode 2 after 20 ns MD: hydrophobic contacts are shown in gray dashed lines, and hydrogen bonds are highlighted in red and (b) Time evolution of hydrogen bond distance between clobenpropit and H4R in mode 2 during 20 ns molecular dynamics. (For interpretation of the references to color in this figure legend, the reader is referred to the web version of the article.)

Phe[7.39]. However, our results show that Glu[5.20] from ECL2 in H4R interacts with clobenpropit, which corresponds to His[5.20] in H3R. Our results also show that Thr[6.55] is unique in H4R and directly interacts with clobenpropit which corresponds to Met[6.55] in H3R. In recent studies [50,56], Thr[6.55] has been reported as an important selectivity residue. These two different but important residues involved in the binding pocket of H4R, contribute to the selectivity of H4R, while the corresponding residues including His[5.20] and Met[6.55] in H3R may also relate to the selectivity of H3R.

Our docking results of clobenpropit with H3R or with H4R are supported by mutation results and preliminary docking results [21,23,53–55,60]. Our results indicate critical differences between the binding pocket in H3R and in H4R, which includes Glu/His[5.20] and Thr/Met[6.55]. The Glu[5.20] not only forms hydrogen bond with clobenpropit, but also influences the binding pocket in H4R, while His[5.20] in H3R does not. Position 6.55 in H4R is Thr[6.55] which is unique in H4R, while the residue in H3R is Met[6.55].

3.5. Molecular dynamics study of complex of H1R with doxepin or histamine

During 20 ns molecular dynamics, the total energy of the system is equilibrated within 6 ns as shown in Fig. S5. 20 ns is a reasonable time scale for our purpose to compare the differences for H1R with different ligands bound.

Our molecular dynamics results show that two important residues: Asp[3.32] and Tyr[3.33] directly interact with doxepin (Fig. 5a). Fig. 5b shows the time evolution for the hydrogen bond distances of them.

Asp[3.32] in H1R forms a stable salt bridge with doxepin during 20 ns MD. Tyr[3.33] tightly interacts with ligand during our MD. Our results show that the complex of H1R and doxepin is stable during our MD.

Similar as the complex of H1R with doxepin, we performed 20 ns MD simulation of complex H1R with histamine with lipid and water. We also find that important residues form stable interactions with ligand during 20 ns MD, as shown in Fig. 6.

Fig. 6c illustrates that the hydrogen bond distance of Asp[3.32] and the protonated ethylamine of ligand keeps stable during our simulation. The hydrogen bond distance between Ser[3.36] and the ligand is stable at 2–4 Å. Asn[5.46] tightly interacts with the imidazole −NH at the first 6 ns, and Thr[3.37] forms a hydrogen bond with the imidazole −NH (Fig. 6a). However, the imidazole −NH moves toward to Thr[5.43] and forms hydrogen bond with Thr[5.43] (keep stable after 6 ns in Fig. 6b). These results indicate that histamine has the flexibility to interact with H1R with different H-bond partners (Fig. 6d).

In the complex of H1R bound with doxepin or histamine, Asp[3.32] always forms strong salt bridge with the ligand, which is important for H1R's function.

3.6. Molecular dynamics study of two mainly different binding poses in H4R

In order to further validate our binding modes of H4R, we performed 20 ns MD simulation of two different modes of the complex H4R-clobenpropit. We find that the total energy of the system is equilibrated within 6 ns as shown in Fig. S6.

Fig. 7a and b shows hydrogen bonds formed between clobenpropit and H4R in two different binding modes after 20 ns MD.

The hydrogen bond distance between the imidazole −NH and Asp[3.32] fluctuates stronger in mode 1 (top of Fig. 7c, red line). However, our results (top of Fig. 7c, blue line) show that the hydrogen bond distance between Asp[3.32] and the protonated −NH is stable in mode 2.

Meanwhile, the hydrogen bond distance between Glu[5.46] and the imidazole −NH is within 5 Å mostly accompanying with little fluctuation in mode 2 (bottom of Fig. 7c, blue line). Moreover, our results show that the hydrogen bond distance between the protonated −NH and Glu[5.46] fluctuates during the first 7.5 ns in mode 1 (bottom of Fig. 7c, red line).

Our results show that both the protonated −NH tightly interacts with receptor. However, in the second mode (mode 2), our results show that the second mode is more stable and more reasonable. Especially the hydrogen bond distance between Asp[3.32] and ligand remains stable.

Jojart et al. [52,54,55] also studied the activation mechanism of H4R by using molecular dynamics simulations with the binding mode that is similar to mode 1. However, in their simulations, they found that the hydrogen bond distance between Glu[5.46] and the protonated ethylamine was stable; while the hydrogen bond between the imidazole −NH of histamine and Asp[3.32] was broken (this hydrogen bond is also broken after 22 ns in our simulation, more detail can be found in Fig. S7).

Based on our second binding mode (mode 2), our results (Fig. 8a and b) show that Glu[5.20] (Glu[165]) tightly interacts with the ligand. The hydrogen bond distance between Glu[5.20] and −N2 is stable (Fig. 8b). Importantly, our results also show that the Thr[6.55] interacts tightly with −Cl of ligand, which is the unique residue existing in H4R and contributes to the selectivity of H4R.

In conclusion, our docking results and MD results of clobenpropit with H4R show that our second binding mode (mode 2) is more reasonable. Glu[5.20] forms hydrogen bond with ligand and keeps stable. Thr[6.55] is unique in H4R also tightly interacts with ligand. These two residues play a key role in the selectivity of H4R.
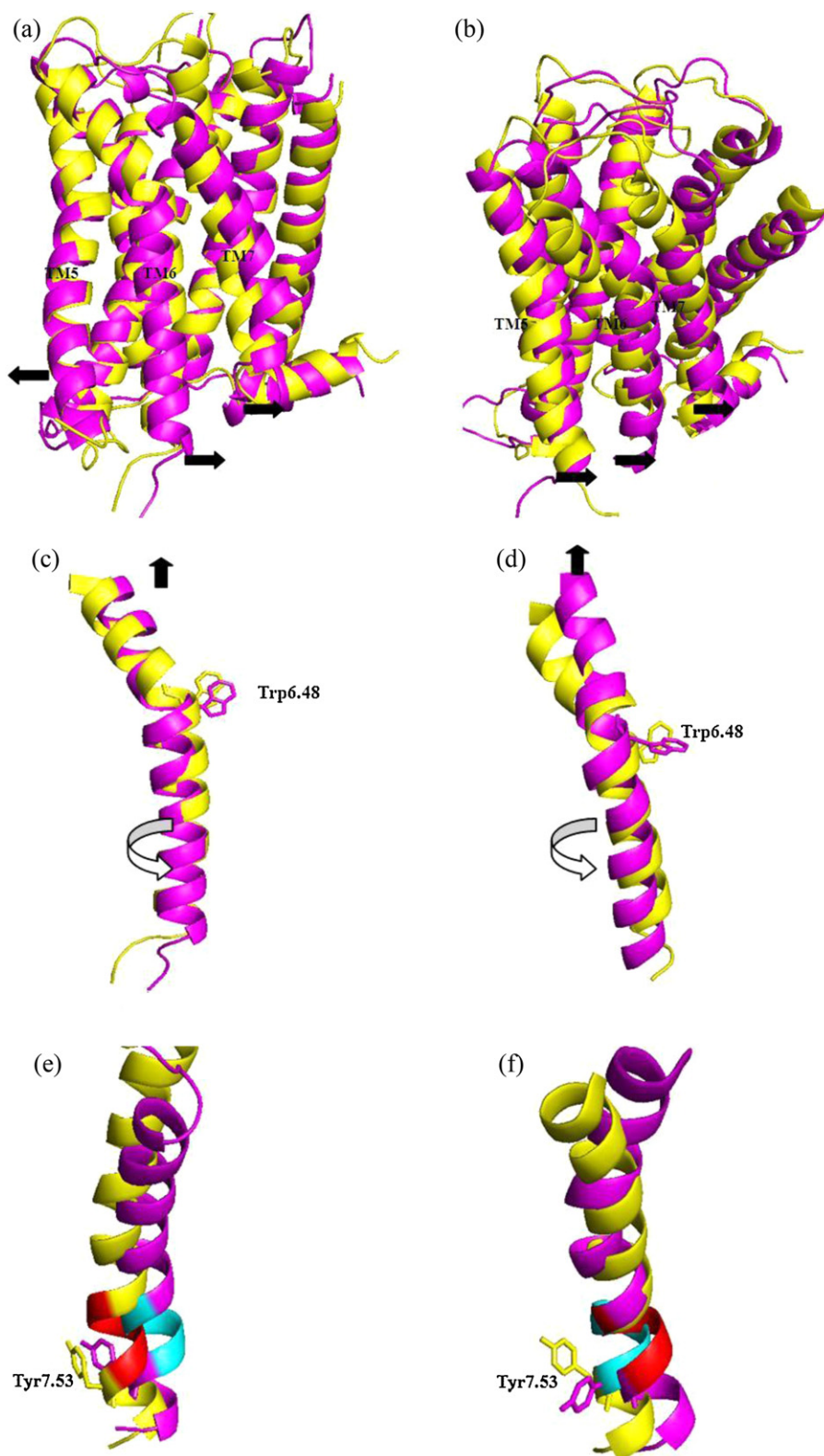
Fig. 9. (a) Comparison of the agonist-bound with antagonist-bound in H1R. The magenta one is the agonist-bound, and the yellow one is the antagonist-bound. The arrow indicates movement of TM5, TM6, and TM7 in H1R with agonist bound. (b) Comparison of the agonist-bound with antagonist-bound in H4R. The magenta one is the agonist-bound, and the yellow one is the antagonist-bound. The arrow indicates movement of TM5, TM6, and TM7 in H4R with agonist bound. (c) Side chain rotamer caused by the rotation and upward-movement of TM6 in H1R. The magenta one is the agonist-bound, and the yellow one is the antagonist-bound. The arrow indicates movement of TM6 in H1R with agonist bound. (d) Side chain rotamer caused by the rotation and upward-movement of TM6 in H4R. The magenta one is the agonist-bound, and the yellow one is the antagonist-bound. The arrow indicates movement of TM6 in H4R with agonist bound. (e) Side view of the rotameric switch of conserved motif "NPXXY" in H1R. The magenta one (or blued) is the agonist-bound, and the yellow one (or red) is the antagonist-bound and (f) Side view of the rotameric switch of conserved motif "NPXXY" in H4R. The magenta one (or red) is the agonist-bound, and the yellow one (or blue) is the antagonist-bound. (For interpretation of the references to color in this figure legend, the reader is referred to the web version of the article.)

3.7. Comparison between agonist-bound and antagonist-bound after MD

We make comparison between agonist-bound and antagonist-bound in H1R and H4R to illustrate the structural information during the activation of histamine receptors.

We first measure the agonist-bound and antagonist-bound MD conformations different from the original crystal structure. The RMSDs of agonist-bound and antagonist-bound MD conformations of H1R with respect to the original crystal structure are 3.02 Å and 1.93 Å, respectively. Moreover, the RMSDs of each conformation of H4R with respect to the homolog model are 3.49 Å and 2.28 Å, respectively. Both agonist-bound MD conformations make significant conformational changes.

During 20 ns MD, TM1, TM2, and TM4 do not make significant deviations as described in other GPCRs [61–64,71,72], while TM3, TM5, TM6 and TM7 make dramatics conformational changes:

(1) Movements of TM5, TM6, and TM7. Our results (Fig. 9a and b) show that the intracellular side of TM6 not only in agonist-bound-H1R, but also in agonist-bound-H4R moves outward. Meanwhile, we find that TM7 both in agonist-bound-H1R and in agonist-bound-H4R moves outward. These similarities between H1R and H4R show that these two receptors share some similarities. However, we find that TM5 in agonist-bound-H1R is far away from TM6, while TM5 in agonist-bound-H4R gets close to TM6. We align the sequences of TM5 both of H1R and of H4R, and find that the sequence identity of TM5 is only 21.9%, while the sequence identity for TM6 and TM7 is 35.3% and 45.8%, respectively. TM5 shows the diversity while TM6 and TM7 show universality during activation.

(2) Side chain rotamer caused by the rotation and upward-movement (toward to the extracellular) of TM6. As shown in Fig. 9c and d, a large change is affected by a small clockwise rotation and upward-movement (toward to extracellular) of TM6 both in H1R and in H4R. $Trp^{6.48}$ is highly conserved in GPCRs, and it has been proposed that its rotameric state is important in activation [61–64,71,72]. Our molecular dynamics illustrates no change in the side chain rotamer of $Trp^{6.48}$ in H1R, which agrees with the recent mutagenesis experiments on the study of crystal structure of $A_{2A}AR$ [61,62,73] and β_2 [74]. However, in H4R, we find that $Trp^{6.48}$ make dramatic conformational change between antagonist-bound and agonist-bound. The reason might be that H4R is obtained based on the crystal structure of H1R, and $Trp^{6.48}$ regulates itself to more preferable states during our MD, which is similar to the finding of Simpson in β_2 [74].

(3) Conformational change of $Tyr^{7.53}$. Conformational changes in TM7 are also important message of activation mechanism [61,62,71,72]. $Tyr^{7.53}$, which belongs to highly conserved NPxxY motif, has a dramatic conformational change ($\sim$2.6 Å in agonist-bound-H1R and $\sim$3.0 Å in agonist-bound-H4R), which has been implicated in the activation mechanism of GPCRs [61,62,71]. Meanwhile, our molecular dynamics results show that the backbone of NPxxY motif makes strong conformational changes ($\sim$2.8 Å in agonist-bound-H1R and $\sim$2.0 Å in agonist-bound-H4R). Comparing Fig. 9e and f, our results show that $Tyr^{7.53}$ in agonist-bound-H4R has stronger conformational change, which may relate to the differences of role and function between H1R and H4R.

All these similarities and differences between H1R and H4R with agonist and antagonist are in agreement with the recent studies of activation mechanism [61–64,71–75], providing more information for the conformational transformations from inactive state to active state, and help us understand the activation mechanism of GPCRs.

4. Conclusion

Based on the recent available high resolution structure of human H1R, we generate homology models of other two subtypes including H3R and H4R. We first dock ligand clobenpropit into H4R based on the crystal structure of H1R and find two mainly different bind modes. In order to select a reasonable binding mode, we dock several other ligands including agonists and antagonists into H4R, and we find that all ligands share a preferable binding mode: the protonated part tightly interacts with $Asp^{3.32}$ while the imidazole $-NH$ of ligand interacts with $Glu^{5.46}$. Moreover, comparing with clobenpropit with H3R, $Glu^{5.20}$ (Glu^{165}) and $Thr^{6.55}$ in H4R contribute to the selectivity of H4R. Then we perform molecular dynamics (MD) of receptors with their compounds bound in explicit lipid and water. Our MD results indicate that our preferable docking mode (mode 2) is more stable. Residue $Glu^{5.20}$ (Glu^{165}) and $Thr^{6.55}$ in H4R potentially relate to the selectivity of H4R. Finally, we dock the agonists to the receptors and compare the conformational changes between agonist-bound and antagonist-bound both of H1R and H4R. Conformational changes in H1R and H4R include: (1) outward movement of intracellular part of TM6 and outward movement of intracellular part of TM7, (2) side chain rotamer caused by the rotation and upward-movement of TM6, and (3) conformational change of $Tyr^{7.53}$, which are consistent with recent reported crystal structures of activated GPCRs. Our results reveal the mechanism of selectivity and activation for H1R/H4R, which is important for developing high selective antagonists and agonists for H1R/H4R.

Acknowledgements

Appendix A. Supplementary data

Supplementary data associated with this article can be found, in the online version, at http://dx.doi.org/ 10.1016/j.jmgm.2012.10.003.

References

[1] M.E. Parsons, C.R. Ganellin, Histamine and its receptors, British Journal of Pharmacology 147 (2006) S127–S135.

[2] C.A. Akdis, F.E. Simons, Histamine receptors are hot in immunopharmacology, European Journal of Pharmacology 533 (2006) 69–76.

[3] S.T. Hong, S. Bang, D. Paik, J. Kang, S. Hwang, K. Jeon, B. Chun, S. Hyun, Y. Lee, J. Kim, Histamine and its receptors modulate temperature-preference behaviors in Drosophila, Journal of Neuroscience 26 (2006) 7245–7256.

[4] L.E. Sander, A. Lorentz, G. Sellge, M. Coeffier, M. Neipp, T. Veres, T. Frieling, P.N. Meier, M.P. Manns, S.C. Bischoff, Selective expression of histamine receptors H1R, H2R, and H4R, but not H3R, in the human intestinal tract, Gut 55 (2006) 498–504.

[5] D. Szukiewicz, G. Szewczyk, J. Klimkiewicz, M. Pyzlak, D. Maslinska, The role of histamine and its receptors in the development of ovarian follicles in vitro, Inflammation Research 55 (2006) S49–S50.

[6] E. Breunig, K. Michel, F. Zeller, S. Seidl, C.W. Weyhern, M. Schemann, Histamine excites neurones in the human submucous plexus through activation of H1, H2, H3 and H4 receptors, Journal of Physiology 583 (2007) 731–742.

[7] E. Zampeli, E. Tiligada, The role of histamine H4 receptor in immune and inflammatory disorders, British Journal of Pharmacology 157 (2009) 24–33.

[8] Y.Y. Li, T.J. Hou, W.A. Goddard, Computational modeling of structure-function of G protein-coupled receptors with applications for drug design, Current Medicinal Chemistry 17 (2010) 1167–1180.

[9] Y. Li, T. Hou, I. Goddard, Computational modeling of structure-function of G protein-coupled receptors with applications for drug design, Current Medicinal Chemistry 17 (2010) 1167–1180.

[10] Y. Li, T. Hou, Computational simulation of drug delivery at molecular level, Current Medicinal Chemistry 17 (2010) 4482–4491.

[11] W.A. Goddard III, S.K. Kim, Y. Li, B. Trzaskowski, A.R. Griffith, R. Abrol, Predicted 3D structures for adenosine receptors bound to ligands: comparison to the crystal structure, Journal of Structural Biology 170 (2010) 10–20.

[12] S.K. Kim, Y. Li, R. Abrol, J. Heo, W.A. Goddard III, Predicted structures and dynamics for agonists and antagonists bound to serotonin 5-HT2B and 5-HT2C receptors, Journal of Chemical Information and Modeling 51 (2011) 420–433.

[13] Y. Li, F. Zhu, N. Vaidehi, W.A. Goddard III, F. Sheinerman, S. Reiling, I. Morize, L. Mu, K. Harris, A. Ardati, Prediction of the 3D structure and dynamics of human DP G-protein coupled receptor bound to an agonist and an antagonist, Journal of the American Chemical Society 129 (2007) 10720–10731.

[14] S.K. Kim, Y. Li, C. Park, R. Abrol, W.A. Goddard III, Prediction of the three-dimensional structure for the rat Urotensin II receptor, and comparison of the antagonist binding sites and binding selectivity between human and rat receptors from atomistic simulations, ChemMedChem 5 (2010) 1594–1608.

[15] S. Fujimoto, M. Komine, M. Karakawa, H. Uratsuji, S. Kagami, Y. Tada, H. Saeki, M. Ohtsuki, K. Tamaki, Histamine differentially regulates the production of Th1 and Th2 chemokines by keratinocytes through histamine H1 receptor, Cytokine 54 (2011) 191–199.

[16] N. Kubo, M. Senda, Y. Ohsumi, S. Sakamoto, K. Matsumoto, M. Tashiro, N. Okamura, K. Yanai, Brain histamine H1 receptor occupancy of loratadine measured by positron emission topography: comparison of H1 receptor occupancy and proportional impairment ratio, Human Psychopharmacology 26 (2011) 133–139.

[17] H.D. Lim, R.M. van Rijn, P. Ling, R.A. Bakker, R.L. Thurmond, R. Leurs, Evaluation of histamine H1-, H2-, and H3-receptor ligands at the human histamine H4 receptor: identification of 4-methylhistamine as the first potent and selective H4 receptor agonist, Journal of Pharmacology and Experimental Therapeutics 314 (2005) 1310–1321.

[18] T. Shimamura, M. Shiroishi, S. Weyand, H. Tsujimoto, G. Winter, V. Katritch, R. Abagyan, V. Cherezov, W. Liu, G.W. Han, T. Kobayashi, R.C. Stevens, S. Iwata, Structure of the human histamine H1 receptor complex with doxepin, Nature 475 (2011) 65–70.

[19] T. Tripathi, A.A. Khan, M. Shahid, H.M. Khan, M. Siddiqui, R.A. Khan, A.A. Mahdi, Immunological, biochemical and histopathological evaluation of histamine receptors (H1R, H2R, H3R and H4R)-antagonist in rabbit experimental model: a short term study, Experimental and Toxicologic Pathology 64 (2010) 259–266.

[20] J.D. Brioni, T.A. Esbenshade, T.R. Garrison, S.R. Bitner, M.D. Cowart, Discovery of histamine H3 antagonists for the treatment of cognitive disorders and Alzheimer's disease, Journal of Pharmacology and Experimental Therapeutics 336 (2010) 38–46.

[21] S. Dastmalchi, M. Hamzeh-Mivehroud, T. Ghafourian, H. Hamzeiy, Molecular modeling of histamine H3 receptor and QSAR studies on arylbenzofuran derived H3 antagonists, Journal of Molecular Graphics and Modelling 26 (2008) 834–844.

[22] M. Ishikawa, T. Furuuchi, M. Yamauchi, F. Yokoyama, N. Kakui, Y. Sato, Synthesis and structure-activity relationships of N-aryl-piperidine derivatives as potent (partial) agonists for human histamine H3 receptor, Bioorganic and Medicinal Chemistry 18 (2010) 5441–5448.

[23] M. Ishikawa, T. Watanabe, T. Kudo, F. Yokoyama, M. Yamauchi, K. Kato, N. Kakui, Y. Sato, Investigation of the histamine H3 receptor binding site. Design and synthesis of hybrid agonists with a lipophilic side chain, Journal of Medicinal Chemistry 53 (2010) 6445–6456.

[24] T. Kottke, K. Sander, L. Weizel, E.H. Schneider, R. Seifert, H. Stark, Receptor-specific functional efficacies of alkyl imidazoles as dual histamine H3/H4 receptor ligands, European Journal of Pharmacology 654 (2011) 200–208.

[25] D. Lazewska, K. Kiec-Kononowicz, Recent advances in histamine H3 receptor antagonists/inverse agonists, Expert Opinion on Therapeutic Patents 20 (2010) 1147–1169.

[26] P. Panula, S. Nuutinen, Histamine and H3 receptor in alcohol-related behaviors, Journal of Pharmacology and Experimental Therapeutics 336 (2010) 9–16.

[27] A. Santillan, K.J. McClure Jr., B.D. Allison, B. Lord, J.D. Boggs, K.L. Morton, A.M. Everson, D. Nepomuceno, M.A. Letavic, A. Lee-Dutra, T.W. Lovenberg, N.I. Carruthers, C.A. Grice, Indole- and benzothiophene-based histamine H3 antagonists, Bioorganic and Medicinal Chemistry Letters 20 (2010) 6226–6230.

[28] B. Schlegel, H. Stark, W. Sippl, H.D. Holtje, Model of a specific human histamine H3 receptor (hH3R) binding pocket suitable for virtual drug design, Inflammation Research 54 (2005) S50–S51.

[29] I.J. de Esch, R.L. Thurmond, A. Jongejan, R. Leurs, The histamine H4 receptor as a new therapeutic target for inflammation, Trends in Pharmacological Sciences 26 (2005) 462–469.

[30] R.A. Smits, M. Adami, E.P. Istyastono, O.P. Zuiderveld, C.M. van Dam, F.J. de Kanter, A. Jongejan, G. Coruzzi, R. Leurs, I.J. de Esch, Synthesis and QSAR of quinazoline sulfonamides as highly potent human histamine H4 receptor inverse agonists, Journal of Medicinal Chemistry 53 (2010) 2390–2400.

[31] R.L. Thurmond, P.J. Desai, P.J. Dunford, W.P. Fung-Leung, C.L. Hofstra, W. Jiang, S. Nguyen, J.P. Riley, S. Sun, K.N. Williams, J.P. Edwards, L. Karlsson, A potent and selective histamine H4 receptor antagonist with anti-inflammatory properties, Journal of Pharmacology and Experimental Therapeutics 309 (2004) 404–413.

[32] N. Terzioglu, R.M. van Rijn, R.A. Bakker, I.J. De Esch, R. Leurs, Synthesis and structure–activity relationships of indole and benzimidazole piperazines as histamine H(4) receptor antagonists, Bioorganic and Medicinal Chemistry Letters 14 (2004) 5251–5256.

[33] E.M. Rosethorne, S.J. Charlton, Agonist-biased signaling at the histamine H4 receptor: JNJ7777120 recruits β-arrestin without activating G proteins, Molecular Pharmacology 79 (2011) 749–757.

[34] D. Studio, Version 2.5, Accelrys Inc., San Diego, CA, USA, 2007.

[35] M. Wiederstein, M.J. Sippl, ProSA-web: interactive web service for the recognition of errors in three-dimensional structures of proteins, Nucleic Acids Research 35 (2007) W407–W410.

[36] R.A. Laskowski, J.A.C. Rullmann, M.W. MacArthur, R. Kaptein, J.M. Thornton, AQUA and PROCHECK-NMR: programs for checking the quality of protein structures solved by NMR, Journal of Biomolecular NMR 8 (1996) 477–486.

[37] E.F. Pettersen, T.D. Goddard, C.C. Huang, G.S. Couch, D.M. Greenblatt, E.C. Meng, T.E. Ferrin, UCSF Chimera—a visualization system for exploratory research and analysis, Journal of Computational Chemistry 25 (2004) 1605–1612.

[38] A.D. MacKerell, D. Bashford, M. Bellott, R.L. Dunbrack, J.D. Evanseck, M.J. Field, S. Fischer, J. Gao, H. Guo, S. Ha, D. Joseph-McCarthy, L. Kuchnir, K. Kuczera, F.T.K. Lau, C. Mattos, S. Michnick, T. Ngo, D.T. Nguyen, B. Prodhom, W.E. Reiher, B. Roux, M. Schlenkrich, J.C. Smith, R. Stote, J. Straub, M. Watanabe, J. Wiorkiewicz-Kuczera, D. Yin, M. Karplus, All-atom empirical potential for molecular modeling and dynamics studies of proteins, Journal of Physical Chemistry B 102 (1998) 3586–3616.

[39] B.R. Brooks, R.E. Bruccoleri, B.D. Olafson, CHARMM: a program for macromolecular energy, minimization, and dynamics calculations, Journal of Computational Chemistry 4 (1983) 187–217.

[40] S.E. Feller, A.D. MacKerell, An improved empirical potential energy function for molecular simulations of phospholipids, Journal of Physical Chemistry B 104 (2000) 7510–7515.

[41] J. Hsin, A. Arkhipov, Y. Yin, J.E. Stone, K. Schulten, Using VMD: an introductory tutorial, Current Protocols in Bioinformatics 7 (2008) 1–5.

[42] W.L. Jorgensen, J. Chandrasekhar, J.D. Madura, R.W. Impey, M.L. Klein, Comparison of simple potential functions for simulating liquid water, Journal of Chemical Physics 79 (1983) 926.

[43] Z. Feng, T. Hou, Y. Li, Studies on the interactions between β2 adrenergic receptor and Gs protein by molecular dynamics simulations, Journal of Chemical Information and Modeling 52 (2012) 1005–1014.

[44] L. Kalé, R. Skeel, M. Bhandarkar, R. Brunner, A. Gursoy, N. Krawetz, J. Phillips, A. Shinozaki, K. Varadarajan, K. Schulten, NAMD2: greater scalability for parallel molecular dynamics* 1, Journal of Computational Physics 151 (1999) 283–312.

[45] U. Essmann, L. Perera, M.L. Berkowitz, T. Darden, H. Lee, L.G. Pedersen, A smooth particle mesh Ewald method, Journal of Chemical Physics 103 (1995) 8577–8593.

[46] E. Plesnar, W.K. Subczynski, M. Pasenkiewicz-Gierula, Saturation with cholesterol increases vertical order and smoothes the surface of the phosphatidylcholine bilayer: a molecular simulation study, BBA-Biomembranes 1818 (2012) 520–529.

[47] T. Tripathi, A.A. Khan, M. Shahid, H.M. Khan, M. Siddiqui, R.A. Khan, A.A. Mahdi, A. Malik, Biochemical and histopathological evaluation of histamine receptors (H1R, H2R, H3R and H4R)-agonist in rabbits, Experimental and Toxicologic Pathology (2011).

[48] J. Jeffry, S. Kim, Z.F. Chen, Itch signaling in the nervous system, Physiology 26 (2011) 286–292.

[49] T. Tripathi, M. Shahid, H.M. Khan, R.A. Khan, M. Siddiqui, A.A. Mahdi, The Influence of histamine H1-receptor on liver functions in immunized rabbits, Saudi, Journal of Biosciences 18 (2011) 411–418.

[50] C. de Graaf, A.J. Kooistra, H.F. Vischer, V. Katritch, M. Kuijer, M. Shiroishi, S. Iwata, T. Shimamura, R.C. Stevens, I.J.P. de Esch, Crystal structure-based virtual screening for fragment-like ligands of the human histamine H 1 receptor, Journal of Medicinal Chemistry 54 (2011) 8195–8204.

[51] N. Shin, E. Coates, N.J. Murgolo, K.L. Morse, M. Bayne, C.D. Strader, F.J. Monsma Jr., Molecular modeling and site-specific mutagenesis of the histamine-binding site of the histamine H4 receptor, Molecular Pharmacology 62 (2002) 38–47.

[52] B. Jojart, R. Kiss, B. Viskolcz, G.M. Keseru, Activation mechanism of the human histamine H4 receptor – an explicit membrane molecular dynamics simulation study, Journal of Chemical Information and Modeling 48 (2008) 1199–1210.

[53] A. Jongejan, H.D. Lim, R.A. Smits, I.J. de Esch, E. Haaksma, R. Leurs, Delineation of agonist binding to the human histamine H4 receptor using mutational analysis, homology modeling, and ab initio calculations, Journal of Chemical Information and Modeling 48 (2008) 1455–1463.

[54] R. Kiss, B. Kiss, A. Konczol, F. Szalai, I. Jelinek, V. Laszlo, B. Noszal, A. Falus, G.M. Keseru, Discovery of novel human histamine H4 receptor ligands by large-scale structure-based virtual screening, Journal of Medicinal Chemistry 51 (2008) 3145–3153.

[55] R. Kiss, B. Noszal, A. Racz, A. Falus, D. Eros, G.M. Keseru, Binding mode analysis and enrichment studies on homology models of the human histamine H4 receptor, European Journal of Medical Chemistry 43 (2008) 1059–1070.

[56] E.P. Istyastono, S. Nijmeijer, H.D. Lim, A.C. van de Stolpe, L. Roumen, A.J. Kooistra, H.F. Vischer, I.J.P. de Esch, R. Leurs, C. De Graaf, Molecular determinants of ligand binding modes in the histamine H 4 receptor: linking ligand-based 3D-QSAR models to in silico guided receptor mutagenesis studies, Journal of Medicinal Chemistry 54 (2011) 8136–8147.

[57] K. Palczewski, T. Kumasaka, T. Hori, C.A. Behnke, H. Motoshima, B.A. Fox, I. Le Trong, D.C. Teller, T. Okada, R.E. Stenkamp, M. Yamamoto, M. Miyano,

Crystal structure of rhodopsin: a G protein-coupled receptor, Science 289 (2000) 739–745.

[58] C. Liu, X. Ma, X. Jiang, S.J. Wilson, C.L. Hofstra, J. Blevitt, J. Pyati, X. Li, W. Chai, N. Carruthers, T.W. Lovenberg, Cloning and pharmacological characterization of a fourth histamine receptor (H(4)) expressed in bone marrow, Molecular Pharmacology 59 (2001) 420–426.

[59] B. Schlegel, C. Laggner, R. Meier, T. Langer, D. Schnell, R. Seifert, H. Stark, H.D. Holtje, W. Sippl, Generation of a homology model of the human histamine H(3) receptor for ligand docking and pharmacophore-based screening, Journal of Computer-Aided Molecular Design 21 (2007) 437–453.

[60] P. Igel, R. Geyer, A. Strasser, S. Dove, R. Seifert, A. Buschauer, Synthesis and structure–activity relationships of cyanoguanidine-type and structurally related histamine H4 receptor agonists, Journal of Medicinal Chemistry 52 (2009) 6297–6313.

[61] G. Lebon, T. Warne, P.C. Edwards, K. Bennett, C.J. Langmead, A.G.W. Leslie, C.G. Tate, Agonist-bound adenosine A(2A) receptor structures reveal common features of GPCR activation, Nature 474 (2011), 521–U154.

[62] F. Xu, H.X. Wu, V. Katritch, G.W. Han, K.A. Jacobson, Z.G. Gao, V. Cherezov, R.C. Stevens, Structure of an agonist-bound human A(2A) adenosine receptor, Science 332 (2011) 322–327.

[63] S.G.F. Rasmussen, B.T. DeVree, Y.Z. Zou, A.C. Kruse, K.Y. Chung, T.S. Kobilka, F.S. Thian, P.S. Chae, E. Pardon, D. Calinski, J.M. Mathiesen, S.T.A. Shah, J.A. Lyons, M. Caffrey, S.H. Gellman, J. Steyaert, G. Skiniotis, W.I. Weis, R.K. Sunahara, B.K. Kobilka, Crystal structure of the beta(2) adrenergic receptor-Gs protein complex, Nature 477 (2011) 549–555.

[64] S.G.F. Rasmussen, H.J. Choi, J.J. Fung, E. Pardon, P. Casarosa, P.S. Chae, B.T. DeVree, D.M. Rosenbaum, F.S. Thian, T.S. Kobilka, A. Schnapp, I. Konetzki, R.K. Sunahara, S.H. Gellman, A. Pautsch, J. Steyaert, W.I. Weis, B.K. Kobilka, Structure of a nanobody-stabilized active state of the beta(2) adrenoceptor, Nature 469 (2011), 175–U59.

[65] E.Y.T. Chien, W. Liu, Q.A. Zhao, V. Katritch, G.W. Han, M.A. Hanson, L. Shi, A.H. Newman, J.A. Javitch, V. Cherezov, R.C. Stevens, Structure of the human dopamine D3 receptor in complex with a D2/D3 selective antagonist, Science 330 (2010) 1091–1095.

[66] B. Wu, E.Y. Chien, C.D. Mol, G. Fenalti, W. Liu, V. Katritch, R. Abagyan, A. Brooun, P. Wells, F.C. Bi, D.J. Hamel, P. Kuhn, T.M. Handel, V. Cherezov, R.C. Stevens, Structures of the CXCR4 chemokine GPCR with small-molecule and cyclic peptide antagonists, Science 330 (2010) 1066–1071.

[67] H.D. Lim, E.P. Istyastono, A. van de Stolpe, G. Romeo, S. Gobbi, M. Schepers, R. Lahaye, W.M.B.P. Menge, O.P. Zuiderveld, A. Jongejan, Clobenpropit analogs as dual activity ligands for the histamine H3 and H4 receptors: synthesis, pharmacological evaluation, and cross-target QSAR studies, Bioorganic and Medicinal Chemistry 17 (2009) 3987–3994.

[68] H.D. Lim, C. de Graaf, W. Jiang, P. Sadek, P.M. McGovern, E.P. Istyastono, R.A. Bakker, I.J.P. de Esch, R.L. Thurmond, R. Leurs, Molecular determinants of ligand binding to H4R species variants, Molecular Pharmacology 77 (2010) 734–743.

[69] M. Wijtmans, C. de Graaf, G. de Kloe, E.P. Istyastono, J. Smit, H. Lim, R. Boonnak, S. Nijmeijer, R.A. Smits, A. Jongejan, Triazole ligands reveal distinct molecular features that induce histamine H4 receptor affinity and subtly govern H4/H3 subtype selectivity, Journal of Medicinal Chemistry 54 (2011) 1693–1703.

[70] M. Wiecek, T. Kottke, X. Ligneau, W. Schunack, R. Seifert, H. Stark, J. Handzlik, K. Kiec-Kononowicz, N-alkenyl and cycloalkyl carbamates as dual acting histamine H3 and H4 receptor ligands, Bioorganic and Medicinal Chemistry 19 (2011) 2850–2858.

[71] T. Warne, R. Moukhametzianov, J.G. Baker, R. Nehme, P.C. Edwards, A.G.W. Leslie, G.F.X. Schertler, C.G. Tate, The structural basis for agonist and partial agonist action on a beta(1)-adrenergic receptor, Nature 469 (2011) 241–244.

[72] J. Standfuss, P.C. Edwards, A. D'Antona, M. Fransen, G.F. Xie, D.D. Oprian, G.F.X. Schertler, The structural basis of agonist-induced activation in constitutively active rhodopsin, Nature 471 (2011) 656–660.

[73] V. Isberg, T. Balle, T. Sander, F.S. Jørgensen, D.E. Gloriam, G protein- and agonist-bound serotonin 5-HT(2A) receptor model activated by steered molecular dynamics simulations, Journal of Chemical Information and Modeling 51 (2011) 315–325.

[74] L.M. Simpson, I.D. Wall, F.E. Blaney, C.A. Reynolds, Modeling GPCR active state conformations: the beta(2)-adrenergic receptor, Proteins 79 (2011) 1441–1457.

[75] H.W. Choe, Y.J. Kim, J.H. Park, T. Morizumi, E.F. Pai, N. Krauss, K.P. Hofmann, P. Scheerer, O.P. Ernst, Crystal structure of metarhodopsin II, Nature 471 (2011) 651–655.